

Recursive Nonlinear Filtering for Angular Data Based on Circular Distributions

Gerhard Kurz¹, Igor Gilitschenski¹, and Uwe D. Hanebeck¹

Abstract—Estimation of circular quantities is a widespread problem that occurs in many tracking and control applications. Commonly used approaches such as the Kalman filter, the extended Kalman filter (EKF), and the unscented Kalman filter (UKF) do not take periodicity explicitly into account, which can result in low estimation accuracy. We present a filtering algorithm for angular quantities in nonlinear systems that is based on circular statistics. The new filter switches between three different representations of probability distributions on the circle, the wrapped normal, the von Mises, and a Dirac mixture density. It can be seen as a systematic generalization of the UKF to circular statistics. We evaluate the proposed filter in simulations and show its superiority to conventional approaches.

I. INTRODUCTION

Estimation of directional quantities is a widespread problem in many tracking and control applications. For example, applications involving moving objects such as cars, ships, planes, spacecraft, or humans usually require estimation of the direction the considered object is facing. Other uses of directional filtering include control of robotic rotary joints and calculation of the relative orientation of several sensors in the process of calibration. Depending on the application, only a single angle in 2D or a complete 3D orientation might be considered.

Currently, it is common to use traditional filters such as the Kalman filter [1] and its nonlinear versions such as the extended Kalman filter (EKF) and the unscented Kalman filter (UKF) [2] for directional filtering (for example [3], [4], [5]). However, these filters are unable to handle directional information explicitly, since they assume that both state and measurements can be represented in \mathbb{R}^n . This leads to issues with the inherent periodicity of directional values. Typical problems include strong dependence on the quality of the initial estimate and failure of the tracking when the discontinuity between 0 and 2π (or at $\pm\pi$, depending on parameterization) is reached. In order to better describe directional information, the use of projected Gaussian distributions has been suggested [6].

Directional statistics [7] allows a correct description of probability distributions on the circle and other manifolds such as spheres or tori. In the past, directional statistics has mostly been used for geographical and biological applications. Considering circular distributions is also of interest for tracking applications [8].

¹ G. Kurz, I. Gilitschenski, and U. D. Hanebeck are with the Intelligent Sensor-Actuator-Systems Laboratory (ISAS), Institute for Anthropomatics, Karlsruhe Institute of Technology, Germany (e-mail: gerhard.kurz@kit.edu, gilitschenski@kit.edu, uwe.hanebeck@ieee.org).

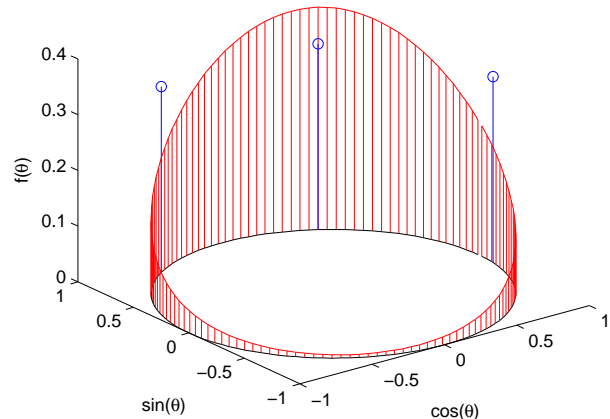


Fig. 1. Wrapped normal distribution with parameters $\mu = 1, \sigma = 1$ and its wrapped Dirac mixture approximation with three components.

Azmani et. al have recently proposed a circular filter based on the von Mises distribution [9]. This filter allows the estimation of a single angle for a system whose system and measurement function are the identity disturbed by additive noise. We present a similar approach based on the wrapped normal and von Mises distributions. The measurement model is required to be the identity with additive noise, but unlike the filter proposed in [9], our filter can be used with a nonlinear system model.

In the next section, we introduce some important probability distributions on the circle and discuss their properties. In Sec. III our circular filter is derived. A simulated example is given in Sec. IV, where a magnetometer is used for correction of noisy gyroscope measurements. In this simulation, we compare the proposed filter with the classical UKF and a slightly modified UKF adapted to a circular setting. Our work is concluded in Sec. V.

II. PROBABILITY DISTRIBUTIONS ON A CIRCLE

Probability distributions on the circle can be understood as the subset of all probability distributions on \mathbb{R} with support $[0, 2\pi)$. An example of such a probability distribution is depicted in Fig. 1. Classical concepts, such as the expected value, statistical dispersion, and limit theorems have to be adapted to the circular situation.

The first *circular moment* (sometimes referred to as *trigonometric moment*) is the circular equivalent to the expected value. For a random variable X taking values in $[0, 2\pi)$, the n -th circular moment is defined as the complex

number

$$\mathbf{E}(e^{inX}) = \int_0^{2\pi} e^{inx} f(x) dx \in \mathbb{C} .$$

As a complex number is composed of two real values, the first circular moment is an analogue to the first two conventional moments of X . The argument $\arg(\mathbf{E}(e^{inX})) \in [0, 2\pi)$ can be seen as the circular mean, whereas the magnitude $|\mathbf{E}(e^{inX})| \in [0, 1]$ is a measure of concentration.

For the development of an angular filter, we introduce two popular continuous distributions on the circle, the wrapped normal distribution and the von Mises distribution. A comprehensive discussion of these distributions can be found in [7] and [10].

We also make use of a Dirac mixture distribution on the circle. A wrapped Dirac mixture with L components and Dirac positions $\beta_1, \dots, \beta_L \in [0, 2\pi)$ is defined as

$$f(x) = \sum_{j=1}^L \omega_j \cdot \delta(x - \beta_j) ,$$

where ω_j are weighting coefficients and $\sum_{j=1}^L \omega_j = 1$. Its n -th circular moment is given by $\mathbf{E}(e^{inX}) = \sum_{j=1}^L \omega_j e^{in\beta_j}$.

A. Wrapped Normal Distribution

The wrapped normal (WN) distribution is the circular version of the normal distribution on the real line. It arises by cutting the normal distribution into intervals of length 2π and additively concentrating it on the interval $[0, 2\pi)$. The probability density function (pdf) of a WN distribution is given by

$$f(\theta) = \frac{1}{\sigma\sqrt{2\pi}} \sum_{k=-\infty}^{\infty} \exp\left(-\frac{(\theta - \mu + 2\pi k)^2}{2\sigma^2}\right) ,$$

where $\theta \in [0, 2\pi)$ with parameters $\mu \in [0, 2\pi)$ and $\sigma \in \mathbb{R}_+$. An example of a WN distribution is depicted in Figure 1.

This distribution is of particular interest, because it is the limit distribution in a circular central limit theorem (which can also be generalized to other manifolds [11]). Consider i.i.d. random variables θ_i with $\mathbf{E}(\theta_i) = 0$ and $\mathbf{E}(\theta_i^2) = \hat{\sigma}^2$. If $\hat{\sigma}^2 < \infty$, then the summation scheme

$$S_n = \frac{1}{\sqrt{n}} \sum_{k=1}^n \theta_k$$

converges to a normally distributed random variable for $n \rightarrow \infty$ and $S_n \bmod 2\pi$ converges to a wrapped normal distributed random variable. Thus, many phenomena arising in nature can be approximated by a WN distribution.

The WN distribution is closed under convolution (i.e., the sum of WN distributed random variables is itself a WN distributed random variable). In contrast to the unwrapped case, the product of two WN densities is not a rescaled WN density. Thus, it is not possible to adapt the classical Kalman filter to the circular case in a straightforward manner.

The n -th circular moment of the WN distribution is given by $\mathbf{E}(e^{inX}) = e^{in\mu - n^2\sigma^2/2}$. Since the first circular moment is a complex number, it is sufficient to completely characterize a WN distribution.

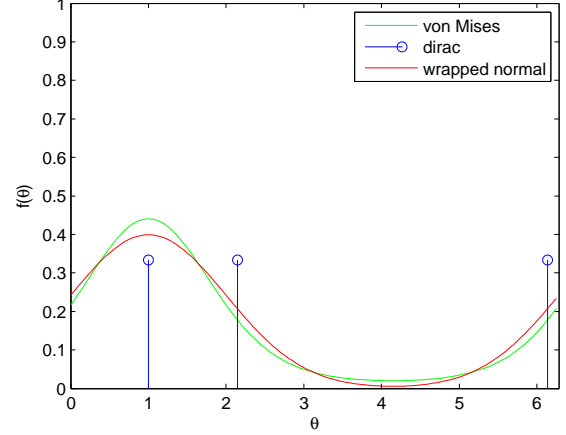


Fig. 2. WN distribution with $\mu = 1, \sigma = 1$ and its VM and Dirac approximations.

B. Von Mises Distribution

The von Mises (VM) distribution is often used as an approximate replacement of a WN distribution. It has a similar shape, while being easier to handle, since its pdf does not involve an infinite sum. The pdf is given by

$$g(\theta) = \frac{1}{2\pi I_0(\kappa)} e^{\kappa \cos(\theta - \mu)} ,$$

where $\theta \in [0, 2\pi)$ and $I_0(x)$ denotes the Bessel-I function of order zero (see [12]). In this representation, $\mu \in [0, 2\pi)$ is a location parameter and $\kappa \in \mathbb{R}_+$ is a concentration parameter. The n -th moment is given by $\mathbf{E}(e^{inX}) = e^{in\mu} I_n(\kappa)/I_0(\kappa)$. Similar to the WN distribution, the first circular moment is sufficient for a full characterization of a VM distribution. Thus, circular moment matching can be used for the conversion between WN, VM, and wrapped Dirac mixture distributions.

III. CIRCULAR FILTER

In this section, we introduce approximations of WN distributions and VM distributions with wrapped Dirac mixtures and vice versa. All approximations rely on circular moment matching, i.e., the first circular moment is preserved when converting between the three different types of distributions. An example of all three distribution types with the same first circular moments is depicted in Fig. 2. Based on these approximations, we present a one-dimensional filter that allows estimation of circular quantities with nonlinear system models and direct measurements in the presence of WN distributed noise.

It deserves mentioning that there is no circular analogue to a filter for linear systems as linearity is a concept of vector spaces rather than manifolds. Any linear map T has to be compatible with scalar multiplication [13], i.e., $T(c \cdot v) = c \cdot T(v)$ for any scalar c and any vector v . This implies $T(0) = T(c \cdot 0) = c \cdot T(0)$ for every scalar c and thus $T(0)(1 - c) = 0$. It follows for $c \neq 1$ that $T(0) = 0$. Unlike a vector space, a manifold – in our case a circle – in general does not have any distinct point zero (the origin) that needs to be mapped to itself by a linear function.

A. Dirac Mixture Approximation of WN Distribution

1) *WN* \rightarrow *Dirac Mixture*: We consider a WN distribution with parameters μ and σ . This distribution is approximated by a wrapped Dirac mixture

$$f^d(x) = \frac{1}{3}\delta(x - (\mu - \alpha)) + \frac{1}{3}\delta(x - \mu) + \frac{1}{3}\delta(x - (\mu + \alpha))$$

with three components. Its parameter α is chosen by matching the first circular moment of the WN distribution

$$\begin{aligned} & \exp\left(in\mu - \frac{n^2\sigma^2}{2}\right) \\ &= \frac{1}{3}\exp(in(\mu - \alpha)) + \frac{1}{3}\exp(in(\mu)) + \frac{1}{3}\exp(in(\mu + \alpha)) . \end{aligned}$$

We solve for α

$$\begin{aligned} \Rightarrow 3 \exp\left(-\frac{n^2\sigma^2}{2}\right) &= \exp(-in\alpha) + 1 + \exp(in\alpha) \\ &= 2 \cos(n\alpha) + 1 \end{aligned}$$

$$\Rightarrow \frac{3}{2} \exp\left(-\frac{n^2\sigma^2}{2}\right) - \frac{1}{2} = \cos(n\alpha)$$

and for $n = 1$, we obtain

$$\alpha = \arccos\left(\frac{3}{2} \exp\left(-\frac{\sigma^2}{2}\right) - \frac{1}{2}\right) .$$

2) *Dirac Mixture* \rightarrow *WN*: For a given wrapped Dirac mixture

$$f(x) = \sum_{j=1}^L \omega_j \delta(x - \beta_j)$$

with L components and weights $\omega_1, \dots, \omega_L$, we obtain the parameters of the corresponding WN distribution by calculating μ as the circular mean

$$\mu = \text{atan2}\left(\sum_{j=1}^L \sin(\beta_j), \sum_{j=1}^L \cos(\beta_j)\right) ,$$

i.e., the argument of the first circular moment, and by matching the first circular moment to obtain σ

$$\begin{aligned} & \exp\left(in\mu - \frac{n^2\sigma^2}{2}\right) = \sum_{j=1}^L \omega_j \exp(in\beta_j) \\ \Rightarrow \exp\left(-\frac{n^2\sigma^2}{2}\right) &= \sum_{j=1}^L \omega_j \exp(in(\beta_j - \mu)) \\ \Rightarrow -\frac{n^2\sigma^2}{2} &= \log\left(\sum_{j=1}^L \omega_j \exp(in(\beta_j - \mu))\right) \\ \Rightarrow \sigma^2 &= -\frac{2}{n^2} \log\left(\sum_{j=1}^L \omega_j \exp(in(\beta_j - \mu))\right) . \end{aligned}$$

For $n = 1$, we have

$$\sigma = \sqrt{-2 \log\left(\sum_{j=1}^L \omega_j \exp(i(\beta_j - \mu))\right)}$$

and with $\sum_{j=1}^L \omega_j \exp(i(\beta_j - \mu)) \in \mathbb{R}$, we reduce this to a real-valued equation

$$\sigma = \sqrt{-2 \log\left(\sum_{j=1}^L \omega_j \cos(\beta_j - \mu)\right)} .$$

B. Dirac-Approximation of VM Distribution

1) *VM* \rightarrow *Dirac Mixture*: Similar to the WN distribution, a VM distribution can be approximated by a wrapped Dirac mixture

$$f^d(x) = \frac{1}{3}\delta(x - (\mu - \alpha)) + \frac{1}{3}\delta(x - \mu) + \frac{1}{3}\delta(x - (\mu + \alpha))$$

as well. For a given VM Distribution with parameters μ and κ , we match the first circular moment

$$\begin{aligned} & \frac{I_n(\kappa)}{I_0(\kappa)} \exp(in\mu) = \\ & \frac{1}{3} \exp(in(\mu - \alpha)) + \frac{1}{3} \exp(in\mu) + \frac{1}{3} \exp(in(\mu + \alpha)) \\ \Rightarrow 3 \frac{I_n(\kappa)}{I_0(\kappa)} &= \exp(-in\alpha) + 1 + \exp(in\alpha) \\ &= 2 \cos(n\alpha) + 1 \\ \Rightarrow \frac{1}{2} \left(3 \frac{I_n(\kappa)}{I_0(\kappa)} - 1\right) &= \cos(n\alpha) \end{aligned}$$

and obtain for $n = 1$

$$\alpha = \arccos\left(\frac{3}{2} \frac{I_1(\kappa)}{I_0(\kappa)} - \frac{1}{2}\right) .$$

2) *Dirac Mixture* \rightarrow *VM*: For a given wrapped Dirac mixture

$$f(x) = \sum_{j=1}^L \omega_j \delta(x - \beta_j)$$

with L components and weights $\omega_1, \dots, \omega_L$, we determine the parameters of the corresponding VM distribution by calculating μ as the circular mean

$$\mu = \text{atan2}\left(\sum_{j=1}^L \sin(\beta_j), \sum_{j=1}^L \cos(\beta_j)\right)$$

like we did for the WN distribution and by matching the first circular moment, we obtain κ from

$$\begin{aligned} & \frac{I_n(\kappa)}{I_0(\kappa)} \exp(in\mu) = \sum_{j=1}^L \omega_j \exp(in\beta_j) \\ \Rightarrow \frac{I_n(\kappa)}{I_0(\kappa)} &= \exp(-in\mu) \sum_{j=1}^L \omega_j \exp(in\beta_j) . \end{aligned}$$

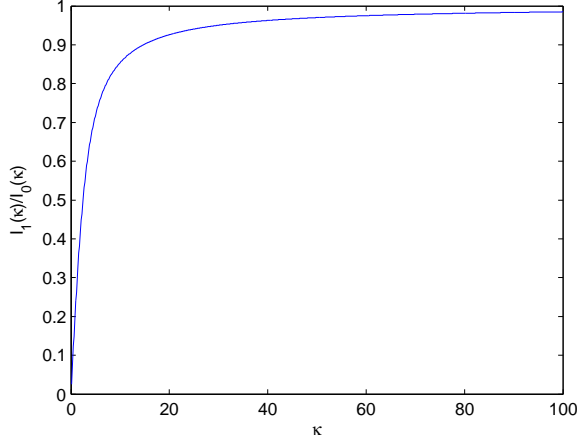


Fig. 3. Ratio of Bessel functions $\frac{I_1(\kappa)}{I_0(\kappa)}$.

For $n = 1$, this yields

$$\frac{I_1(\kappa)}{I_0(\kappa)} = \exp(-i\mu) \sum_{j=1}^L \omega_j \exp(i\beta_j),$$

which can be solved numerically for κ . As can be seen in Fig. 3, this function is not difficult to invert numerically. The Bessel functions $I_1(\kappa)$ and $I_0(\kappa)$ approach infinity very fast even though their ratio $\frac{I_1(\kappa)}{I_0(\kappa)}$ is always a value in the interval $[0, 1]$. To avoid numerical problems, the ratio of Bessel functions should be calculated by the algorithm described in [14] (see Fig. 4).

Input: v, x , number of iterations N , 10 by default

Output: $\frac{I_{v+1}(x)}{I_v(x)}$

```

o ← min(v, 10);
for i ← 0 to N do
  | r(i + 1) ←  $\frac{x}{o+i+0.5+\sqrt{(o+i+1.5)^2+x^2}}$ ;
end
for i ← 1 to N do
  | for k ← 0 to N - i do
  | | r(k + 1) ←  $\frac{x}{o+k+1+\sqrt{(o+k+1)^2+x^2\frac{r(k+2)}{r(k+1)}}}$ ;
  | end
end
y ← r(1);
i ← o;
while i > v do
  | y ←  $\frac{1}{(2i/x+y)}$ ;
  | i ← i - 1;
end
return y;

```

Fig. 4. Algorithm for calculating the ratio of Bessel functions.

C. Conversion of WN and VM

For any given WN distribution, a VM distribution with identical first circular moment can be found and vice versa. This can be done indirectly by conversion to a wrapped Dirac mixture and subsequent conversion to the desired distribution. Both steps retain the first circular moment and can be calculated as described above. However, it is more efficient to directly convert between WN and VM distributions.

Let μ_{WN}, σ_{WN} be the parameters of a WN distribution and μ_{VM}, κ_{VM} the parameters of a VM distribution. Obviously, $\mu_{WN} = \mu_{VM}$ holds for reasons of symmetry. Matching the first circular moment

$$\begin{aligned} \frac{I_n(\kappa_{VM})}{I_0(\kappa_{VM})} \exp(in\mu_{VM}) &= \exp\left(in\mu_{WN} - \frac{n^2\sigma_{WN}^2}{2}\right) \\ \Rightarrow \frac{I_n(\kappa_{VM})}{I_0(\kappa_{VM})} &= \exp\left(-\frac{n^2\sigma_{WN}^2}{2}\right) \end{aligned}$$

yields for $n = 1$

$$\Rightarrow \frac{I_1(\kappa_{VM})}{I_0(\kappa_{VM})} = \exp\left(-\frac{\sigma_{WN}^2}{2}\right).$$

1) $VM \rightarrow WN$: This equation can easily be solved for σ_{WN} , which results in

$$\sigma_{WN} = \sqrt{-2 \log\left(\frac{I_1(\kappa_{VM})}{I_0(\kappa_{VM})}\right)}.$$

2) $WN \rightarrow VM$: Solving the same equation for κ_{VM} is done numerically. Once again, the ratio of Bessel functions should be calculated by the algorithm described in [14] (see Figure 4).

D. Kullback-Leibler Divergence

The Kullback-Leibler divergence of two probability distributions P and Q is a measure of the information lost when P is approximated by Q . It is given by

$$\int P(\theta) \log\left(\frac{P(\theta)}{Q(\theta)}\right) d\theta.$$

As is obvious from its definition, the Kullback-Leibler divergence is not a metric because it lacks symmetry. To illustrate the similarity between the WN and VM distributions, we show the Kullback-Leibler divergence between a WN distribution with given σ and the VM distribution with identical first circular moment (Fig. 5). Due to the fact that we consider conversions between WN and VM distributions in both directions, we also show the converse Kullback-Leibler divergence. Furthermore, we compare the WN distribution to a non-wrapped Gaussian with equal standard deviation. Fig. 5 illustrates the fact that a Gaussian distribution is a poor approximation of a WN distribution for large uncertainties σ . This result further motivates the use of circular distributions.

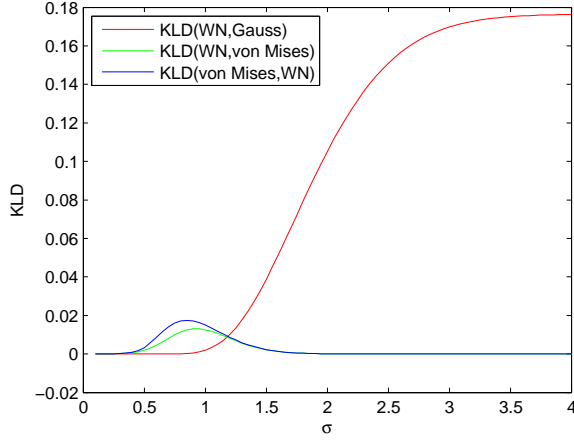


Fig. 5. Kullback-Leibler divergence of the WN distribution with given σ , a Gaussian distribution and the von Mises distribution.

E. Prediction

We consider a system model

$$\theta_{k+1} = a_k(\theta_k) + w_k$$

with state θ_k at time step k , the (possibly nonlinear) system function a_k and additive WN-distributed noise w_k with parameters μ_{w_k}, σ_{w_k} . Prediction occurs by approximating the WN density with a wrapped Dirac mixture, propagating each Dirac component through the system function a_k , approximating the resulting wrapped Dirac mixture with a WN density, and adding the noise w_k by calculating the convolution (Figure 6).

Input: a_k (system function),

μ_k^e, σ_k^e (estimated distribution of state),

μ_{w_k}, σ_{w_k} (distribution of system noise)

Output: μ_k^p, σ_k^p (predicted distribution of state)

```

/* Dirac approximation */
 $\alpha \leftarrow \arccos\left(\frac{3}{2} \exp\left(-\frac{(\sigma_k^e)^2}{2}\right) - \frac{1}{2}\right);$ 
/* application of system function */
 $\beta_1 \leftarrow a_k(\mu_k^e - \alpha);$ 
 $\beta_2 \leftarrow a_k(\mu_k^e);$ 
 $\beta_3 \leftarrow a_k(\mu_k^e + \alpha);$ 
/* conversion of Diracs back to WN */
 $\mu \leftarrow \text{atan2}\left(\sum_{j=1}^3 \sin(\beta_j), \sum_{j=1}^3 \cos(\beta_j)\right);$ 
 $\sigma \leftarrow \sqrt{-2 \log\left(\frac{1}{3} \sum_{j=1}^3 \cos(\beta_j - \mu)\right)};$ 
/* convolution with noise */
 $\mu_k^p \leftarrow (\mu + \mu_{w_k}) \bmod 2\pi;$ 
 $\sigma_k^p \leftarrow \sqrt{\sigma^2 + \sigma_{w_k}^2};$ 

```

Fig. 6. Algorithm for Prediction.

F. Measurement Update

Assume a measurement model

$$\hat{z}_k = \theta_k + v_k$$

with measurement \hat{z}_k , state θ_k and additive WN-distributed noise v_k with parameters μ_{v_k}, σ_{v_k} .

With Bayes' rule, we have

$$f(\theta_k | \hat{z}_k) = c \cdot f(\hat{z}_k | \theta_k) \cdot f(\theta_k)$$

with the normalization constant

$$c = \frac{1}{\int_0^{2\pi} f(\hat{z}_k | \theta_k) \cdot f(\theta_k) d\theta_k}.$$

We calculate $f(\hat{z}_k | \theta_k)$ according to

$$\begin{aligned} f(\hat{z}_k | \theta_k) &= \int_0^{2\pi} f(\hat{z}_k, v_k | \theta_k) dv_k \\ &= \int_0^{2\pi} f(\hat{z}_k | \theta_k, v_k) f^v(v_k) dv_k \\ &= \int_0^{2\pi} \delta(\hat{z}_k - \theta_k - v_k) f^v(v_k) dv_k \\ &= f^v(\hat{z}_k - \theta_k), \end{aligned}$$

where f^v is the distribution of the additive noise v_k . Thus, we obtain the equation

$$f(\theta_k | \hat{z}_k) = c \cdot f^v(\hat{z}_k - \theta_k) f(\theta_k)$$

for the filtered density. Consequently, filtering is done by multiplying the densities $f^v(\hat{z}_k - \theta_k)$ and $f(\theta_k)$ and subsequent renormalization if necessary (Figure 7). Since WN distributions are not closed under multiplication, an intermediate representation of VM distributions is used. Multiplication of two VM distributions and normalization of the resulting density is performed as described in [9].

Input: measurement \hat{z}_k ,

μ_k^p, σ_k^p (predicted distribution of state),

μ_{v_k}, σ_{v_k} (distribution of measurement noise)

Output: μ_k^e, σ_k^e (estimated distribution of state)

```

/* shift  $f^v$  by measurement */
 $\tilde{\mu}_{v_k} \leftarrow (\hat{z}_k - \mu_{v_k}) \bmod 2\pi;$ 
 $\tilde{\sigma}_{v_k} \leftarrow \sigma_{v_k};$ 
/* convert to VM distribution */
 $\mu_1, \kappa_1 \leftarrow \text{wnToVonMises}(\mu_k^p, \sigma_k^p);$ 
 $\mu_2, \kappa_2 \leftarrow \text{wnToVonMises}(\tilde{\mu}_{v_k}, \tilde{\sigma}_{v_k});$ 
/* multiply densities */
 $C \leftarrow \kappa_1 \cos \mu_1 + \kappa_2 \cos \mu_2;$ 
 $S \leftarrow \kappa_1 \sin \mu_1 + \kappa_2 \sin \mu_2;$ 
 $\mu \leftarrow \text{atan2}(S, C);$ 
 $\kappa \leftarrow \sqrt{S^2 + C^2};$ 
/* convert back to WN distribution */
 $\mu_k^e, \sigma_k^e \leftarrow \text{vonMisesToWn}(\mu, \kappa);$ 

```

Fig. 7. Algorithm for measurement update.

IV. SIMULATION

Consider the following example: A robot arm is moved by a single rotary joint. Since the robot arm is affected by gravity, the torque acting on the rotary joint depends on the current angle. The robot arm is observed by some sensor that is capable of measuring the absolute orientation. Our goal is to estimate the angle of the rotary joint.

The system can be modeled by

$$\theta_{k+1} = a_k(\theta_k) + w_k$$

with system function

$$a_k(\theta_k) = \theta_k + \underbrace{c_1 \sin(\theta_k)}_{\text{gravity}} + \underbrace{c_2}_{\text{velocity}},$$

where θ_k is the state and w_k is WN-distributed noise. The constants c_1, c_2 can be derived from a physical model of the system. The measurement equation is given by

$$\hat{z}_k = \theta_k + v_k,$$

where \hat{z}_k is the orientation measurement and v_k is WN-distributed noise.

The noise parameters have been chosen as $\mu_{v_k} = \mu_{w_k} = 0$, $\sigma_{v_k} = 0.1$, $\sigma_{w_k} = 0.1$ and the physical parameters have been chosen as $c_1 = 0.1$, $c_2 = 0.15$. The initial state estimate at time step $k = 0$ is given by $\mu_0^e = 3$, $\sigma_0^e = 2$. The true initial state is given by $\theta_0 = 0$. Obviously, the initial estimate is very poor and has high uncertainty in this example.

We compare our approach with the UKF [2], because it is commonly used in nonlinear estimation problems involving directional quantities. The UKF is based on the assumptions that all occurring probability distributions are Gaussian. Since the UKF does not take into account the periodicity of angular states and measurements, we also consider a modified version of the UKF, where

$$\mu_k \leftarrow \mu_k \bmod 2\pi$$

is enforced after every prediction and update step and

$$\tilde{z}_k \leftarrow \begin{cases} \hat{z}_k, & |\mu_p - z| \leq \pi \\ \hat{z}_k + 2\pi \text{sign}(\mu_p - z), & |\mu_p - z| > \pi \end{cases}$$

is used as a measurement. Because $\hat{z}_k \in [0, 2\pi)$, the modified measurement \tilde{z}_k is always in the range $[\mu_p - \pi, \mu_p + \pi]$.

The results of the simulation over a period of 150 time steps are depicted in Figure 8. Because the discontinuity between 0 and 2π can make a regular two-dimensional plot misleading, we also provide a three-dimensional plot where the angles are depicted as points on a cylinder. Furthermore, plots of the angular error

$$\min(|\hat{\theta}_k - \mu_k^e|, 2\pi - |\hat{\theta}_k - \mu_k^e|)$$

at every time step k are provided. The angular error describes the shorter length of the two possible paths between two points on the circle. It is obvious that the unmodified UKF performs very poorly when it encounters the discontinuity at 2π . The modified UKF and the proposed filter produce good estimates, but the proposed filter achieves smaller 3σ -bounds.

The angular root mean square error (angular RMSE)

$$\sqrt{\frac{1}{150} \sum_{k=1}^{150} \left(\min(|\hat{\theta}_k - \mu_k^e|, 2\pi - |\hat{\theta}_k - \mu_k^e|) \right)^2}$$

of the different filters was calculated for 100 runs and is depicted as a boxplot in Figure 9. As can be seen, the estimation error of the original UKF is very large (mean 0.6135, median 0.5917). The modified UKF is a significant improvement (mean 0.1458, median 0.1448), but does not achieve as good results as our proposed filter (mean 0.0812, median 0.0812). In this example, the mean error of the UKF is 656% higher than the proposed filter and the mean error of the modified UKF is still 80% higher. Even though our filter is computationally somewhat more demanding than the UKF, it is easily fast enough for typical real-time applications.

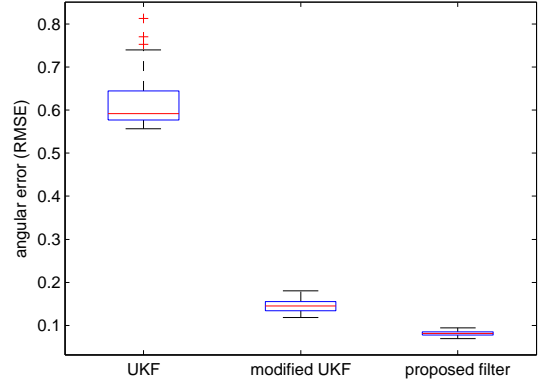


Fig. 9. Angular RMSE over 100 runs, for the proposed filter, the UKF and the modified UKF.

V. CONCLUSION

We have presented a filter for the estimation of angles that can be applied to nonlinear systems. Simulations with a simple example system suggest that the proposed filter is vastly superior to the commonly used UKF in the case of circular estimation problems. Furthermore the proposed filter gives better results than a modified UKF enhanced to handle circular estimation.

Future research might include the estimation of orientations in 3D. In addition, for many practical applications it is desirable to combine the estimation of directional quantities and \mathbb{R}^n -vectors in a single filter, for example for the purpose of 6D pose estimation.

ACKNOWLEDGMENT

This work was partially supported by grants from the German Research Foundation (DFG) within the Research Training Groups RTG 1194 ‘‘Self-organizing Sensor-Actuator-Networks’’ and RTG 1126 ‘‘Soft-tissue Surgery: New Computer-based Methods for the Future Workplace’’.

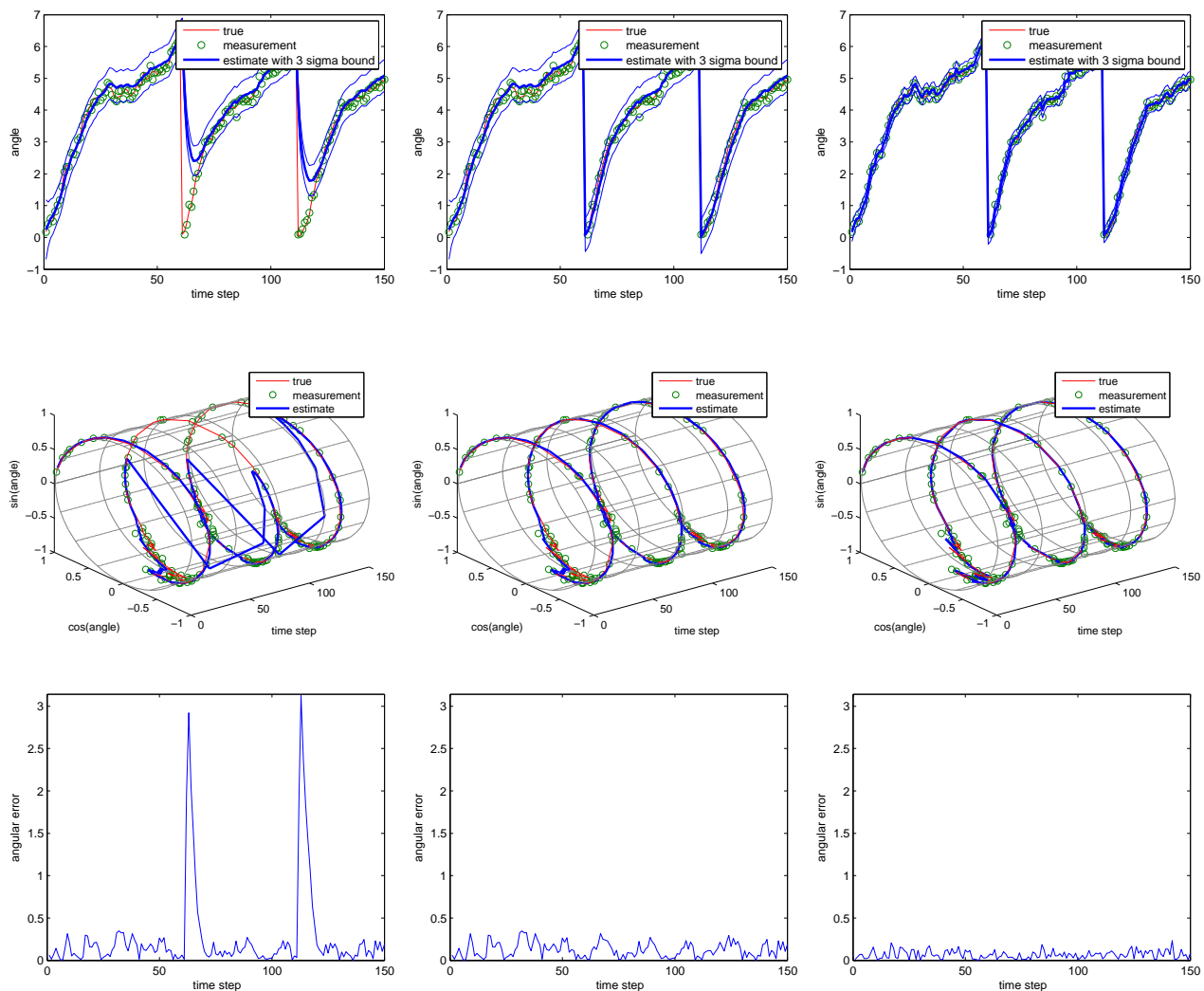


Fig. 8. Simulation results, from left to right: UKF, modified UKF, proposed filter. All angles as well as the angular error are given in radians.

REFERENCES

- [1] R. E. Kalman, "A New Approach to Linear Filtering and Prediction Problems," *Transactions of the ASME Journal of Basic Engineering*, vol. 82, pp. 35–45, 1960.
- [2] S. Julier and J. Uhlmann, "Unscented filtering and nonlinear estimation," *Proceedings of the IEEE*, vol. 92, no. 3, pp. 401–422, mar 2004.
- [3] F. M. Mirzaei and S. I. Roumeliotis, "A kalman filter-based algorithm for imu-camera calibration: Observability analysis and performance evaluation," *IEEE Transactions on Robotics*, vol. 24, no. 5, pp. 1143–1156, 2008.
- [4] A. Bry, A. Bachrach, and N. Roy, "State estimation for aggressive flight in gps-denied environments using onboard sensing," in *Proc. IEEE Int Robotics and Automation (ICRA) Conf*, 2012.
- [5] F. Faion, P. Ruoff, A. Zea, and U. D. Hanebeck, "Recursive Bayesian Calibration of Depth Sensors with Non-Overlapping Views," in *Proceedings of the 15th International Conference on Information Fusion (Fusion 2012)*, Singapore, Jul. 2012.
- [6] W. Feiten and M. Lang, "MPG - a framework for reasoning on 6 dof pose uncertainty," in *ICRA 2011 Workshop on Manipulation Under Uncertainty*, Shanghai, China, 2011.
- [7] K. V. Mardia and P. E. Jupp, *Directional Statistics*, 1st ed. Wiley, 1999.
- [8] J. Clark, R. Vinter, and M. Yaqoob, "The shifted rayleigh filter for bearings only tracking," in *2005 8th International Conference on Information Fusion*, vol. 1, 2005.
- [9] M. Azmani, S. Reboul, J.-B. Choquel, and M. Benjelloun, "A recursive fusion filter for angular data," in *IEEE International Conference on Robotics and Biomimetics (ROBIO)*, 2009, pp. 882–887.
- [10] S. R. Jammalamadaka and A. Sengupta, *Topics in Circular Statistics*. World Scientific Pub Co Inc, 2001.
- [11] K. R. Parthasarathy, "The central limit theorem for the rotation group," *Theory of Probability & Its Applications*, vol. 9, no. 2, pp. 248–257, Jan. 1964.
- [12] M. Abramowitz and I. A. Stegun, Eds., *Handbook of Mathematical Functions: with Formulas, Graphs, and Mathematical Tables*. Dover Publications, 1965.
- [13] M. Artin, *Algebra*. Upper Saddle River, New Jersey: Prentice Hall, 1991.
- [14] D. E. Amos, "Computation of modified bessel functions and their ratios," *Mathematics of Computation*, vol. 28, no. 125, pp. 239–251, 1974.